



HAL
open science

Producing A615 / A615M High Strength Construction Re-Bars Without Use of Microalloys: Part 2

Ignatius C. Okafor, Kaushal R. Prayakarao, Heshmat A. Aglan

► **To cite this version:**

Ignatius C. Okafor, Kaushal R. Prayakarao, Heshmat A. Aglan. Producing A615 / A615M High Strength Construction Re-Bars Without Use of Microalloys: Part 2. *Mechanics, Materials Science & Engineering Journal*, 2015, 10.13140/RG.2.1.2749.2887 . hal-01302025

HAL Id: hal-01302025

<https://hal.science/hal-01302025>

Submitted on 14 Apr 2016

HAL is a multi-disciplinary open access archive for the deposit and dissemination of scientific research documents, whether they are published or not. The documents may come from teaching and research institutions in France or abroad, or from public or private research centers.

L'archive ouverte pluridisciplinaire **HAL**, est destinée au dépôt et à la diffusion de documents scientifiques de niveau recherche, publiés ou non, émanant des établissements d'enseignement et de recherche français ou étrangers, des laboratoires publics ou privés.



Distributed under a Creative Commons Attribution 4.0 International License

Producing A615 / A615M High Strength Construction Re-Bars Without Use of Microalloys: Part 2

Ignatius C. Okafor^{1a}, Kaushal R. Prayakarao^{2a}, Heshmat A. Aglan^{2b}

1 – Chief Metallurgist, Nucor Steel Corporation, Marion OH 43302 USA

a – Ignatius.okafor@nucor.com

2 – Department of Mechanical Engineering, Tuskegee University, Tuskegee, Alabama, USA

a – Kprayakarao2649@mytu.tuskegee.edu

b – Aglanh@mytu.tuskegee.edu

Keywords: A615 high strength steel, re-bar steel (grade 60), rolling process, superheat, metallurgy, grain refinement, microalloys, economical steel.

ABSTRACT. The metallurgy of ASTM A615/A615M Gr. 60 steels made from three different chemistries was studied to suggest an economically advantageous route to produce a steel grade that saves the extra cost of alloying elements. Metallographic examinations, along with microhardness and XRD studies, were performed to rate the steel chemistries based on their superheats. This study of the steel grades revealed that producing steel for requisite standards like ASTM 615/A615M Grade 60 may not be dependent on starting superheat but on the chemistry and rolling process. Study of the three chemistries A, B and C indicated that the standards were met in all 3 chemistries; however, sample A had the lowest cost chemistry and therefore is a suggested route for this product.

1. Introduction. ASTM A615/A615M Grade 60 standard calls for a minimum 60 Ksi (420MPa) yield strength with no upper limit even on tensile strength. The standard only specifies that phosphorus (P) be no more than 0.06%. The resulting plain carbon steel is expected to have basic ferrite – pearlite microstructure with minimum grain size ASTM 5. Because every steel mill is different and processes vary, some steel mills use some microalloying to achieve fine grain size in pursuit of the aim microstructure. This process of compositional and process variations can produce yield strengths typically in the range of 350 to 700 MPa (50 – 100 Ksi). Microalloying, which enhances physical properties through ferritic grain refinement, is often supplemented by precipitation and or dislocation strengthening. Hall-Petch type of strengthening is determined to suggest that a decrease of ferritic grain size from ASTM 6 – 8 to ASTM 12 – 13 is accompanied by an increase of 30 Ksi (210 MPa) in yield strength. Admittedly the other good effect of fine grains besides strengthening is good ductility or toughness.

Two common microalloying elements V and Nb are used in industry to achieve this goal and several authors [1-6] have studied their use. It is known that the behavior of individual micro alloying elements classifies them as mildly carbide forming or strongly carbide forming. The two micro alloying elements (V and Nb) used in this study do qualify as strong carbide formers. They therefore stabilize the α phase. This essentially means that they reduce the γ phase field. Any of the elements in solid solution in α strengthen the ferrite matrix in steel. These elements differ in their contribution to hardening and the extent to which they reduce plasticity as they add a certain increment to strength.

Furthermore, compared to other microalloying elements like Nb and Ti, vanadium exhibits essential differences. The Swedish Institute of Metals Research [6] found that the solubility of vanadium carbonitrides, in particular, is much larger and the solubility of vanadium's nitride is about two orders of magnitude smaller than its carbide, contrary to Nb but similar to Ti. Vanadium has higher solubility in austenite than niobium, and its carbonitrides [V(C,N)] dissolve more easily prior to hot rolling than NbC. Consequently, vanadium is an excellent choice for strong and easily controllable precipitation strengthening, but it is expensive.

Thermodynamically it is known that pure ferrite dissolves more N than C. Thus the total N-content of the steel is normally dissolved in the ferrite before V (C,N) precipitation, whereas only a fraction of the C-content is dissolved in ferrite. Hence the precipitation strengthening would and does increase with total C-content, an effect [6] not previously recognized.

Regarding the Nb containing steel in this study, niobium is known to have three-fold influence on the mechanical properties of steel. It facilitates grain size refinement; lowers the gamma (γ) to alpha (α) transition temperature (Ar_3), and enhances precipitation hardening.

Grain refinement is the only mechanism that increases strength, toughness, and ductility all simultaneously. This makes niobium the most effective microalloying element even when small quantities are added to the steel. The mechanism for grain refinement is mainly due to delaying or preventing recrystallization in the last hot-forming (rolling) steps. Flattened grains associated with the process and the attendant dislocation density of the austenite enhance ferrite nucleation. By lowering the gamma (γ) to alpha (α) transformation temperature, niobium enhances ferrite nucleation and simultaneously reduces grain growth rate. The combined effect yields a very fine grain structure. This is, however, obtainable only when niobium is in solid solution. To achieve niobium in solid solution, an adequate furnace re-heating temperature is essential. At an elevated temperature, Nb(C,N) precipitates before rolling. More Nb(C,N) can precipitate quite easily in austenite under deformation. This is due to the well understood strain induced precipitation. The resulting particles from this process inhibit grain growth and even austenite grain recrystallization during the intermittent deformation at lower temperatures. Deformed austenite structure transforms to fine ferritic structure upon cooling, giving rise to high strength and toughness. Since the Nb carbonitrides are stable at low temperatures, more strength is accomplished as remaining niobium bearing particles precipitate during cooling.

The third steel grade in this study (Fe-Mn-C) does not contain any intentionally added alloying element. Carbon content and elements like Mn and Ni do also stabilize and lower the Ar_3 - temperature. Ni content in the steels studied while not purposely added are appreciably high residuals (0.15 – 0.21Ni). Suppression of gamma to ferrite transformation temperatures is known to enhance refinement of the final structure by decreasing the growth rate of the ferrite grains. Traditionally the major difference in the steels for plate and long products lies in the higher carbon contents of the latter. Pearlite formation in long products is thus greater and does tend to develop bainitic or other acicular microstructures. Besides, the processing of long products necessitates relatively higher finishing temperatures; hence recrystallization controlled rolling (RCR, process 3 in Fig. 1 below) is used in order to obtain a most homogenous fine grain size and high strength in final product.

The purpose of this work is to study the metallurgy of ASTM A615/A615M Gr. 60 steels made from three chemistries and so suggest an economically advantageous route that saves the extra cost of alloying elements. The study is in two parts. The first (Part 1, yet to be submitted) discusses microstructure and the effect of cooling rates on the said chemistries while the second (Part 2; this paper) discusses microstructure, physical properties and centerline segregation.

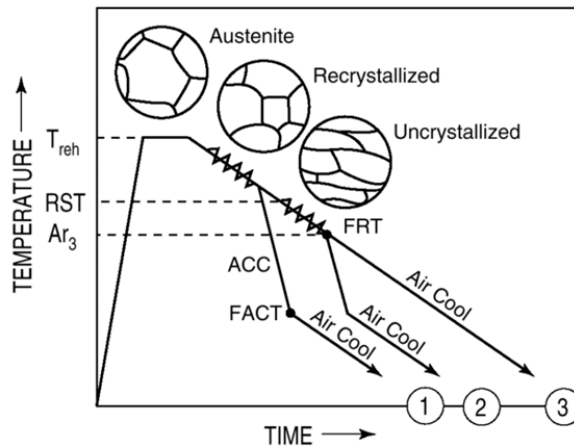


Figure 1. Thermo-mechanical controlled processes (TMCP): 1) recrystallization controlled rolling and accelerated cooling, 2) controlled rolling and accelerated cooling, and 3) recrystallization controlled rolling with air-cooling [6].

2. EXPERIMENTAL PROCEDURE

2.1. Processing of Steels. The steels (A, B, and C) used in this work were melted by an electric-arc-furnace tapped into 60 ton ladles, cast into billets, and rolled into #6 (19 mm) re-bars. The compositions are shown in Table 1. All three steels had identical carbon, manganese, and silicon contents and all other elements besides vanadium and niobium were residuals.

Steel A was specifically made without an intentional addition of vanadium or niobium. The 0.005 V in the chemistry is typical of residual vanadium content in scrap. Steel B was made with an intentional addition of 0.025 V and steel C was made with an intentional addition of 0.012 Nb.

For the purpose of this work the effect of other elements (typically residuals) were not considered. All steels were air cooled on a hot bed at production conditions.

Table 1. Chemical composition of the three alloys used in the study

No Vanadium added (A)		Vanadium Added (B)		Niobium Added (C)	
Cast Temp-Superheat-		Cast Temp-Superheat-		Cast Temp-Superheat-	
Element	Wt%	Element	Wt%	Element	Wt%
C	0.40	C	0.37	C	0.30
Mn	1.06	Mn	0.99	Mn	1.10
S	0.033	S	0.029	S	0.037
P	0.017	P	0.024	P	0.012
Si	0.18	Si	0.18	Si	0.24
Cu	0.48	Cu	0.31	Cu	0.36
Cr	0.22	Cr	0.23	Cr	0.16
Mo	0.06	Mo	0.08	Mo	0.05
Sn	0.013	Sn	0.011	Sn	0.018
Ni	0.21	Ni	0.17	Ni	0.15
Nb	0.000	Nb	0.000	Nb	0.012
V	0.005	V	0.025	V	0.003
Pb	0.000	Pb	0.000	Pb	0.004

2.2. Tensile Strength Prediction Based on Chemistry: (Fe-C-Mn, Fe-C-Mn-Nb, and Fe-C-Mn-V)

Tensile strength for each chemistry studied was calculated using the prediction models available in the literature. The relationship of these chemistries to strength has been made by several authors [7, 8]. In his work, Pickering [1] suggested the following formula for alloys where carbon content is less than 0.25%C.

$$TS \text{ (MPa)} = 243 + 1900C + 228(\text{Cr}+\text{Mn}) + 228\text{Mo} + 91\text{W} + 22\text{Ni} + 61\text{Cu} + 380(\text{Ti} + \text{V})$$

Pickering did not suggest any contribution from silicon.

De Boer [2], however, basing his work on a carbon content of approximately 0.4%C and 1.5%Si, suggested a contribution for silicon as indicated in the following equation.

$$TS \text{ (MPa)} = 430 + 688 + 81 \text{ Si} + 196\text{Mn} + 202\text{Cr} + 80\text{Mo} + 400\text{V}$$

De Boer also tested the influence of Mn (0.70 to 1.3 wt. %), Cr (0.15 to 1.5 wt. %), Mo (0.20 to 0.8 wt. %), and V (0.0 to 0.10 wt. %).

Mesplont [3] and his team, starting from De Boer's work, modified the equation with the use of more elements and developed the following equation.

$$TS \text{ (MPa)} = 288 + 803C + 83\text{Mn} + 178\text{Si} + 122\text{Cr} + 320\text{Mo} + 60\text{Cu} + 180\text{Ti} + 1326\text{P} + 2500\text{Nb} + 360000\text{B}$$

The authors applied this equation to 164 steels; the results are shown in Fig. 2.

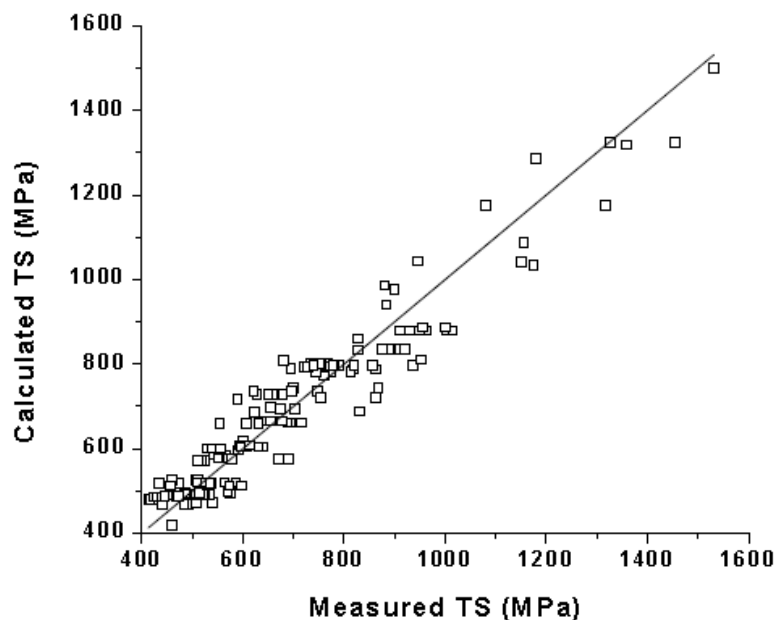


Figure 2. Calculated TS (MPa) versus measured TS (MPa) [3]

Because the elemental chemical analysis of our three alloys falls into the chemistry ranges used by Mesplont and co-workers [3], we have used their equation to “predict” or verify the tensile strengths of the alloys studied.

Steel A

TS (MPa) = $288+803(0.402) +83(1.06) +178(0.18) +122(0.22) +320(0.056) +60(0.482) +180(0) +1326(0.017) + 2500(0.000) +36000(0.0)$. This gives an empirical tensile strength of 120 Ksi. The actual mill measurement for this heat was 110 Ksi; the difference of between 8% and 9% is certainly understandable and of no obvious concern.

Steel B

Sample B calculated tensile strength is 116.6 Ksi while the actual mill result is 112.3 Ksi. As for alloy A, the difference between the theoretical value predicted by Mesplont’s equation and the actual is between 3.7% and 3.8%.

Steel C

Sample C in this study has a calculated tensile strength of 106.67 Ksi while the measured (mill) tensile strength was reported as 96.4 Ksi. The difference is between 9.63 % and 10.68%.

The objective of this exercise is not to verify the accuracy or lack thereof of Mesplont’s equation but to have a common verifiable frame of reference other than mill reports to compare the tensile strengths. The maximum difference of 10 percentage points between calculated and measured values irrespective of the use of alloying elements (which we all know in metallurgy as grain refiners) is truly instructive. It is this closeness that further drove this work where we seek to minimize the use of expensive alloying elements in making some basic grades of carbon steel needed in the construction industry.

2.3. Metallography of Samples

Three sets of samples, each from all three different steels, were mounted using Buehler Simplimet 1000 with Bakelite and polished for light optical metallography, microhardness studies, and SEM work. All samples were polished to the usual mirror image and etched using 2% Nital.

Metallographic pictures obtained from the optical microscopy were then studied for microstructural variations and grain sizes were estimated from the microstructures for each steel grade.

2.4. Microhardness Tests

Microhardness measurements were made on samples that had been polished and etched to reveal microstructure. Hardness was taken for each of the phases identified in the metallography. Microhardness data were obtained from around the center line of the three steel grade studies. Particular attention was paid to the center line to determine if any differences arose from the difference in the superheat experience of the steels during casting. The microhardness data were also calculated using equations (obtained from literature) based on chemistry variations. Calculated and measured results were later compared. Microhardness measurements were made in both rolling (horizontal along the length of the bar) directions and transverse directions (vertically above and below the center line at about ± 5 mm above the center line). Effort was made to measure the contribution (microhardness) of each phase type found in the microstructure. Average hardness of the phases was then found and used for this study.

2.5. Solute Element Distribution

Samples from each steel type studied (A, B and C) were sectioned along the center of the rolled piece, polished but not etched, and then studied in the SEM to find distribution of specific solute elements (C, P, S, and Mn). As in the case of the microhardness studies, the SEM element distribution was also done in two directions, longitudinal and transverse. Element distribution as identified in the SEM were color coded in each case, as discussed in the results.

2.6. Tensile and Yield Strength Measurements

Tensile and yield strengths of the steels were obtained from the mill where they were rolled. All three results met the requirements for ASTM 615/615M specifications for tensile, yield, and elongation.

3. RESULTS AND DISCUSSION

3.1. Microstructural Analysis

Steel A:

Figs. 3 – 5 show the microstructures along the center line of the three different alloys (A, B and C) produced with different superheats (72 deg. F, 142 deg. F and 82 deg. F), respectively. Three microstructural phases, namely ferrite, pearlite (with small amounts of bainite) and grain boundary ferrite (GBF), are seen in all the samples.

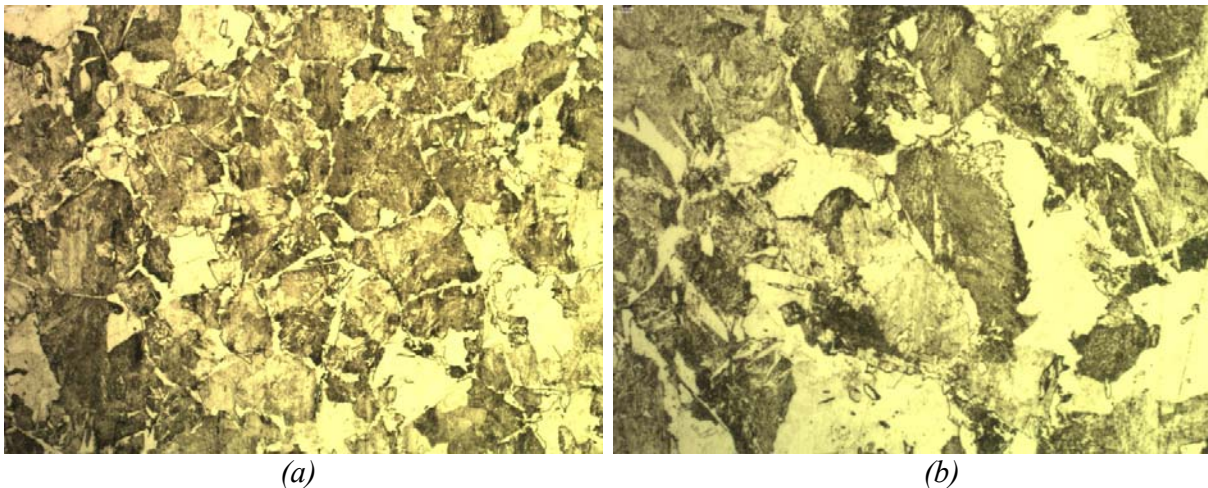


Figure 3. Optical micrographs of alloy A, 72 deg. F superheat, at (a) 20X and (b) 50X magnification

Fig. 3 is the microstructure of the steel sample A, which was made without the addition of any microalloys. It shows mostly ferrite (whitish portions) and pearlite (dark areas) microstructure with little patches of bainitic structure. The average grain diameter meets a minimum of 32 μm (ASTM 7) grain size. Fine grain microstructure is typically defined as meeting ASTM 5 grain size.

Steel B:

Fig. 4 shows the microstructure of Sample B, which was made with addition of 0.025V wt%. It shows evidence of pearlitic and ferritic microstructure with more patches of bainitic microstructure. Grain boundary allotriomorphs are evident growing off the prior austenite grain boundaries. This is more noticeable in Fig. 4 (b), which has a larger magnification. Grain size diameter here is about 16 μm

(ASTM 9), which does meet the fine grain microstructure. This result is expected for vanadium addition to steel.

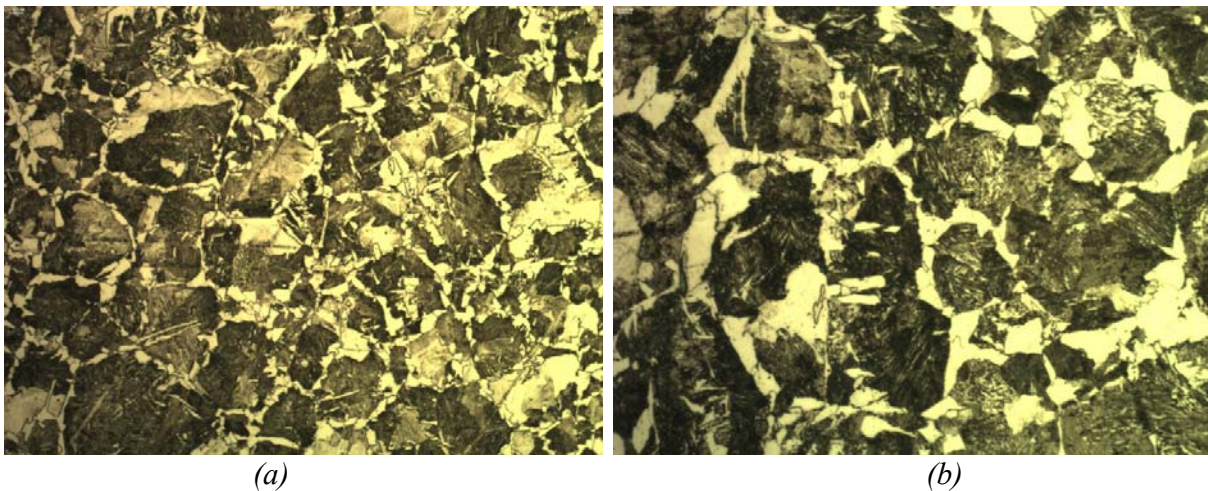


Figure 4. Optical micrographs of alloy B, 142 deg. F superheat, at (a) 20X and (b) 50X magnification

Steel C:

Sample C was made with small addition of niobium; the microstructure shows greater a amount of bainitic structure than the microstructures for samples A and b. Sample C has much lower level of carbon (0.3 wt %) compared to samples A and B, which had carbon around 0.4 wt%. The lower carbon levels take away from the strength but niobium, or microalloying for that matter, compensates for the strength and improves toughness. It is known that addition of Nb gives about twice as much boost in strength as vanadium of the same quantity. Combination of both Nb and V do provide a significant boost in strength [9].

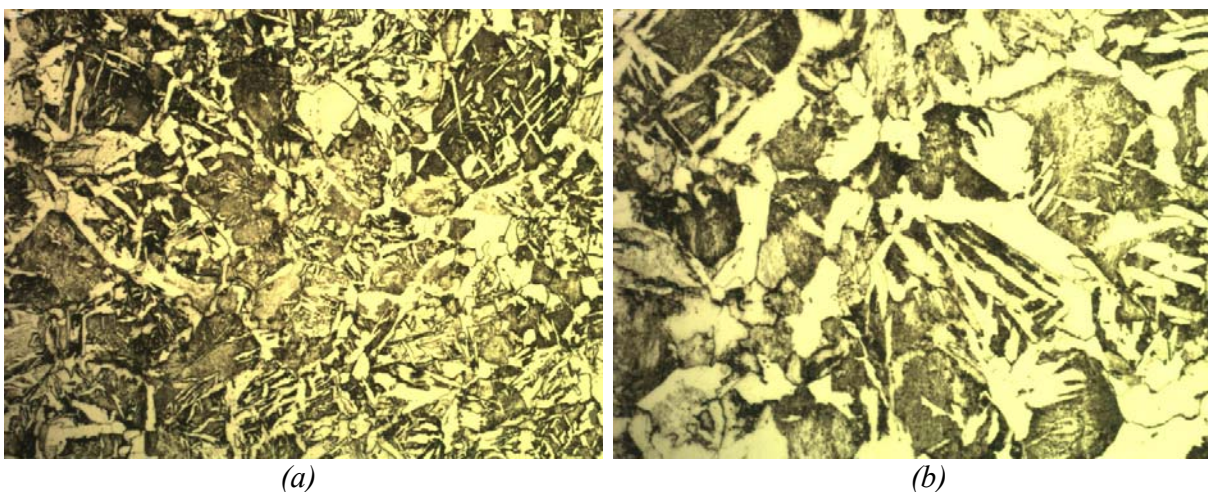


Figure 5. Optical micrographs of alloy C, 82 deg. F superheat, at (a) 20X and (b) 50X magnification

The volume fractions of ferrite and pearlite in the three steels studied are shown in Table 2.

Table 2. Volume fractions of the microstructural phases in different steels

Vol. Fraction %	C (Nb)	B (V)	(No Microalloy)
Avg. Ferrite	11.48%	6.81%	9.17%
Avg. Pearlite	88.52%	93.20%	90.83%

Average bainite is assumed to be no more than 5% in A and B but about 10% in C.

3.2. Microhardness Results

Microhardness of each steel sample (A, B and C) was measured at points indicated in Fig. 6. The dark points represent where the hardness measurements were made. The three horizontal lines represent (from top to bottom) +5mm above the center line; center line, and -5mm below the center line, respectively. Positive and negative signs are used to emphasize top and below the center line, which is presumed to be zero.

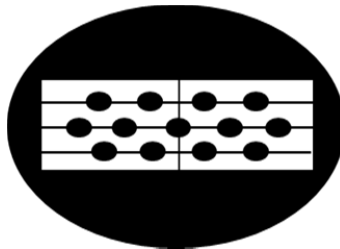


Figure 6. Schematic representation of the locations on the sample surface where microhardness data was obtained

Table 3. Microhardness results for sample A (no vanadium added)

H 72F (No Vanadium)	Phase	-4	-3	-2	-1	0	1	2	3	4	Avg.
+5mm	Ferrite	341		298		271		300		383	319
	Pearlite	382		402		383		374		422	393
	GBF	334		220		295		241		349	288
Center line	F	276	341	326	322	382	365	342	383	402	349
	P	361	390	382	432	387	452	395	392	432	403
	GBF	216	237	241	288	306	341	349	294	327	289
-5mm	F	266		286		334		266		349	300
	P	455		388		357		349		422	394
	GBF	313		228		276		256		341	283

Table 4. Microhardness results for sample B (0.025 wt. %V vanadium added)

SH 142F (V added)	Phase	-4	-3	-2	-1	0	1	2	3	4	Avg
	Ferrite	349		300		365		294		432	348
+5mm	Pearlite	455		357		383		374		506	415
	GBF	341		298		224		266		334	293
	F	282	365	422	479	443	334	349	276	313	363
Centerline	P	455	392	492	486	482	476	402	495	434	457
	GBF	357	247	320	300	327	349	256	276	288	302
	F	374		343		367		341		340	353
-5mm	P	405		389		454		432		412	418
	GBF	313		341		283		276		283	299

Table 5. Microhardness results for sample C (0.0120 wt. % Nb added)

SH 82F(NB added)	Phase	-4	-3	-2	-1	0	1	2	3	4	Avg
	Ferrite	313		313		313		327		288	311
+5mm	Pearlite	392		387		402		402		357	388
	GBF	256		288		282		251		251	266
	F	328	313	288	362	334	412	356	326	361	347
CL	P	412	397	357	432	374	432	383	394	388	397
	GBF	273	290	293	261	306	300	298	289	224	282
	F	288		282		300		288		334	298
-5mm	P	392		349		402		412		374	386
	GBF	251		237		276		276		288	266

The results in Tables 3-5 indicate that the hardness varies from 266 in the GBF of sample C to 457 at the center line of sample B. While this dispersion may appear significant the broad spectrum, the averages of the results suggest that the samples all meet the required hardness.

3.3. Solute Elements Distribution across the Center Line (Horizontal)

X-ray diffraction (XRD) analysis was performed on the samples along the center line (horizontally) to determine solute (C, P, S, and Mn) distribution pattern in those axes. A typical sample probe axis is shown in Fig. 7.

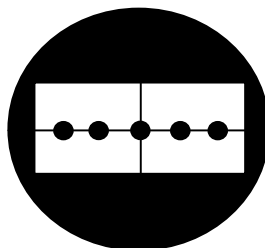


Figure 7. Schematic of the sample used in the solute distribution probe

Plot of the solute element distribution in the sample as determined by SEM is shown in Fig. 8 for sample A. The distribution is made for relative concentration (wt. %) against spatial location in the x-direction. The sample was 1.5” long.

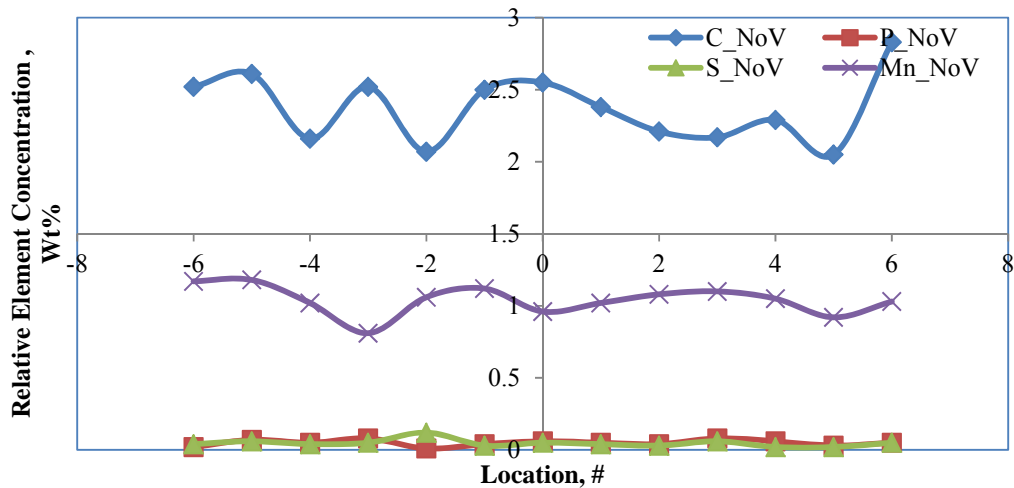


Figure 8. Solute element relative concentration against spatial location for sample A (no vanadium)

Fig. 8 is presented such that points above the horizontal line are from the upper half of the sample center line, while the lower portion is below the line. It is instructive to observe that P and S were mostly traced at the center line, while not much Mn was noted there, but rather at some noticeable distance above the center line. It should be noted that all efforts to find the exact center line in the finished rolled material used in the study was not successful when using a SEM.

A similar distribution profile was observed for sample B, which had some intentional vanadium addition (Fig. 9).

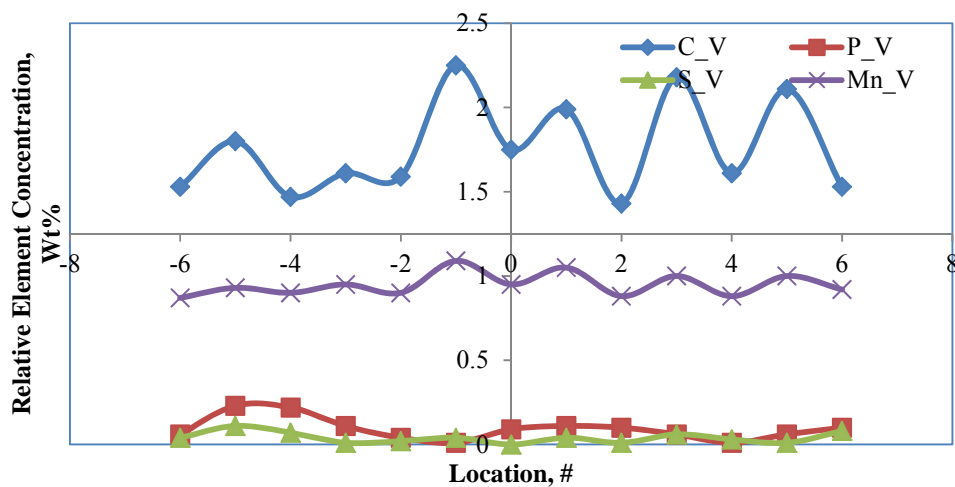


Figure 9. Solute element relative concentration against spatial location for sample B (vanadium added)

As for sample A, S and P are found along the center line while C and Mn are detected significantly above the center line. No effort is made to determine the exact quantities of these elements since our machine is limited in that capability; hence we report only the relative values.

Fig. 10 shows the findings for sample C (niobium added). These results are comparable to those for samples A and B.

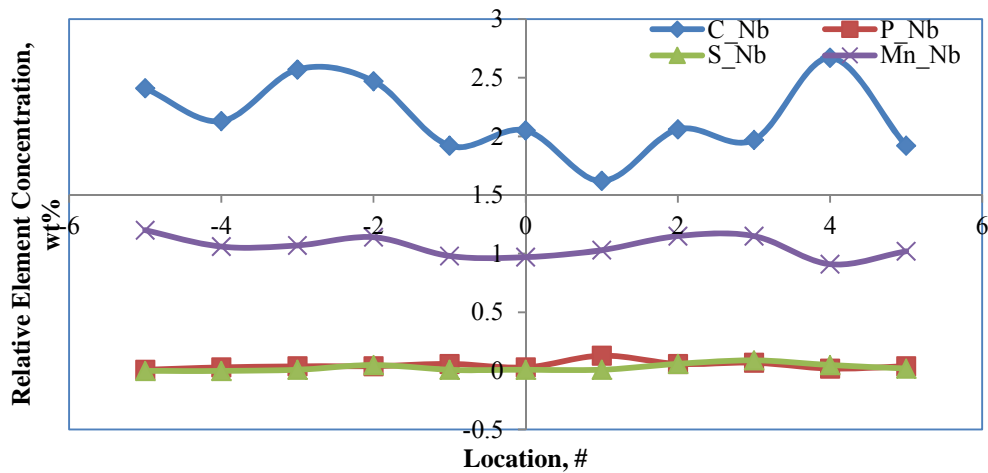


Figure 10. Solute element relative concentration against spatial location for sample C (Nb added)

3.4. Solute Elemental Distribution (vertical direction)

Similar solute distribution profiles were run in the vertical direction as indicated in Fig. 11.

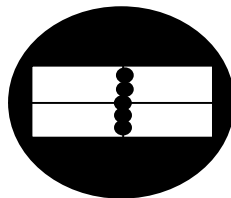


Figure 11. Schematic of the vertical direction (black dots)

Relative element distribution for sample A, which had no intentional vanadium addition, is given in Fig. 12. The distribution is along the vertical axis. Except for the small spike in carbon, the elements seem to distribute evenly along the bar. The right of the graph represent points above the center line (+Y directions) and the left represent the points below the center line (- Y direction)

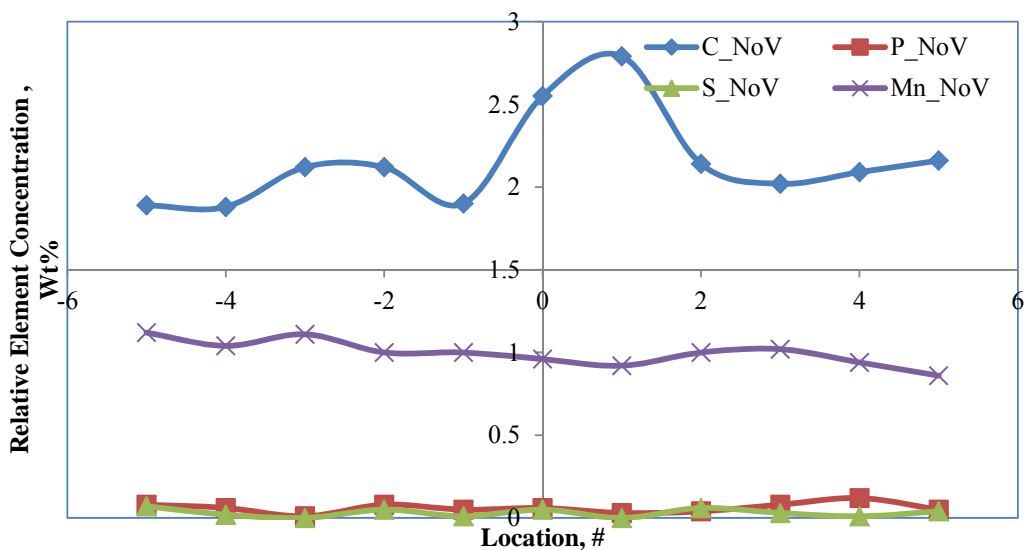


Figure 12. Solute element distribution in the vertical direction for sample A (no vanadium added)

An identical profile run for sample B (vanadium added) is presented in Fig. 13. As for the sample A profile, the right of Fig. 13 (+Y direction) represents points above the center line and the left represent the points below the center line (- Y direction).

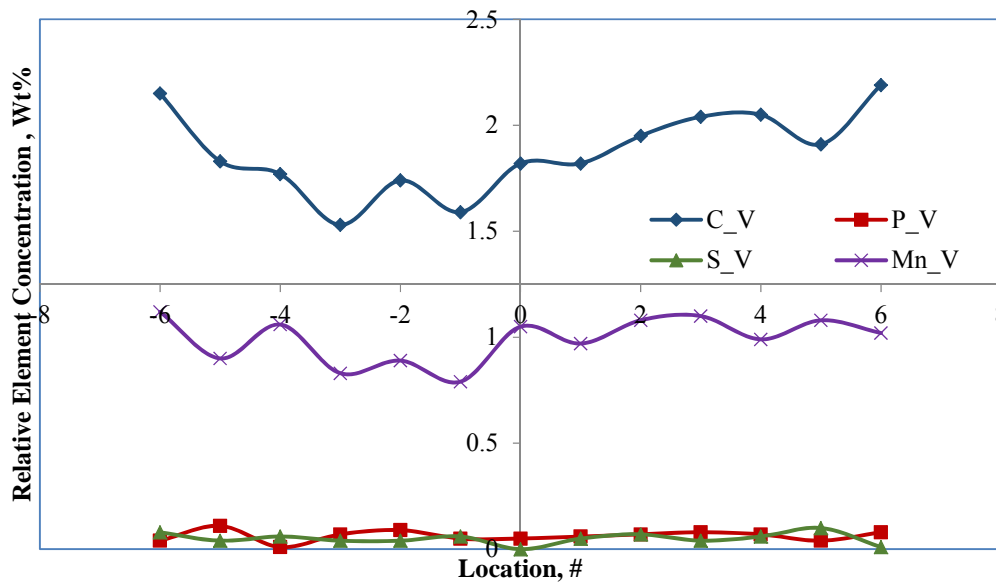


Figure 13. Solute element distribution in the vertical direction for sample B (vanadium added, superheat 142⁰F)

The distribution of Mn, S and P all seem rather uniform; the carbon profile is somewhat non-linear yet not clustered. It does not show the carbon hump observed in the no vanadium alloy, sample A.

A third vertical distribution curve is shown in Fig. 14 for the niobium added alloy, sample C.

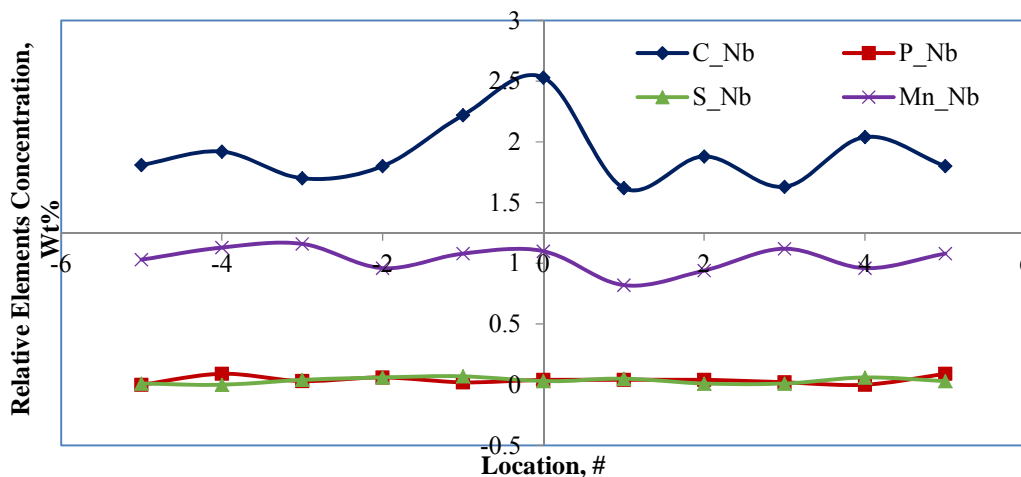


Figure 14. Solute element distribution in the vertical direction for sample C (niobium added, superheat 82⁰ F)

As for sample A with no vanadium addition, this profile shows a slight carbon hump, while exhibiting some uniformity in the distribution of other solute elements traced.

3.5. Scanning Electron Microscopy Studies of the Center Line

The center line of the samples was subjected to SEM examination to see if any “openings” would be detected in any of the three samples studied. Such “openings” would suggest center line decohesion and so signal physical property weakness. The purpose of the different superheats used in this study is essentially enable visibility of any such decohesion if it exists. The results are shown in Figs. 15-17.

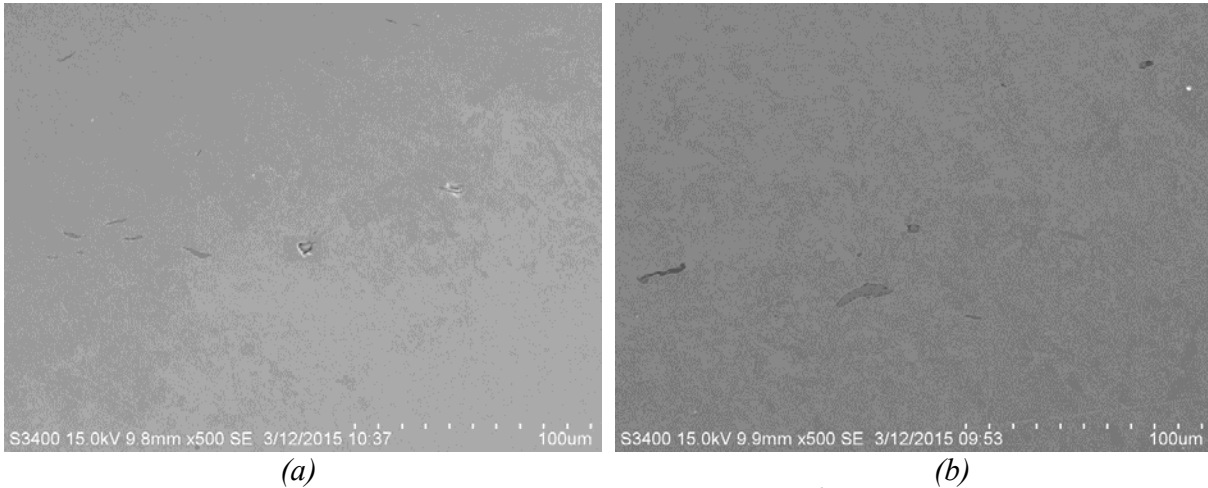


Figure 15. SEM micrographs of sample A (no-vanadium) with 72⁰ F superheat; 500X magnification.

The SEM micrographs show typical heterogeneities /inclusions across the center line but no “open” center line decohesion.

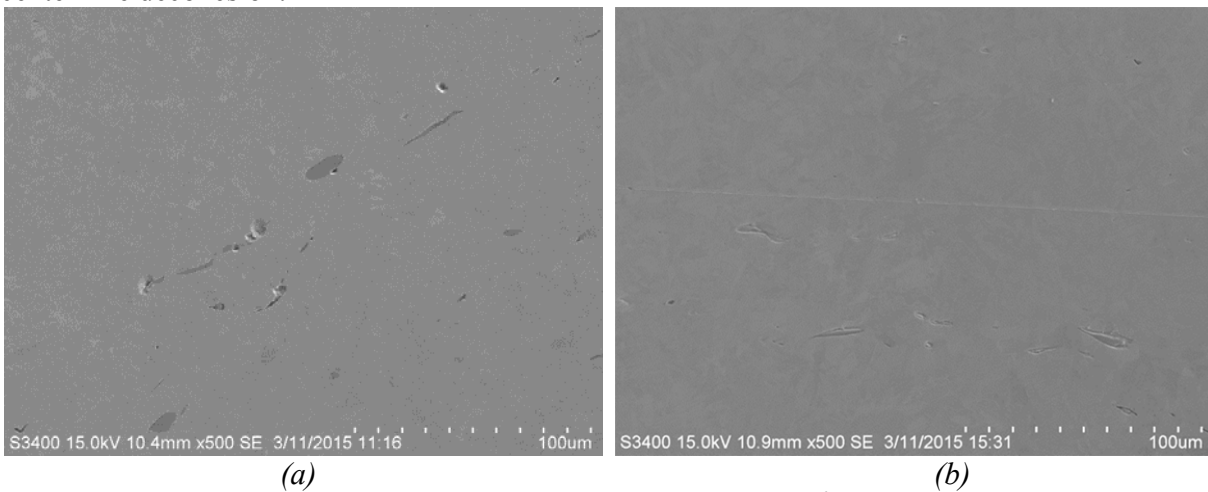


Figure 16. SEM micrographs of sample B (vanadium added), 142⁰ F superheat; 500X magnification

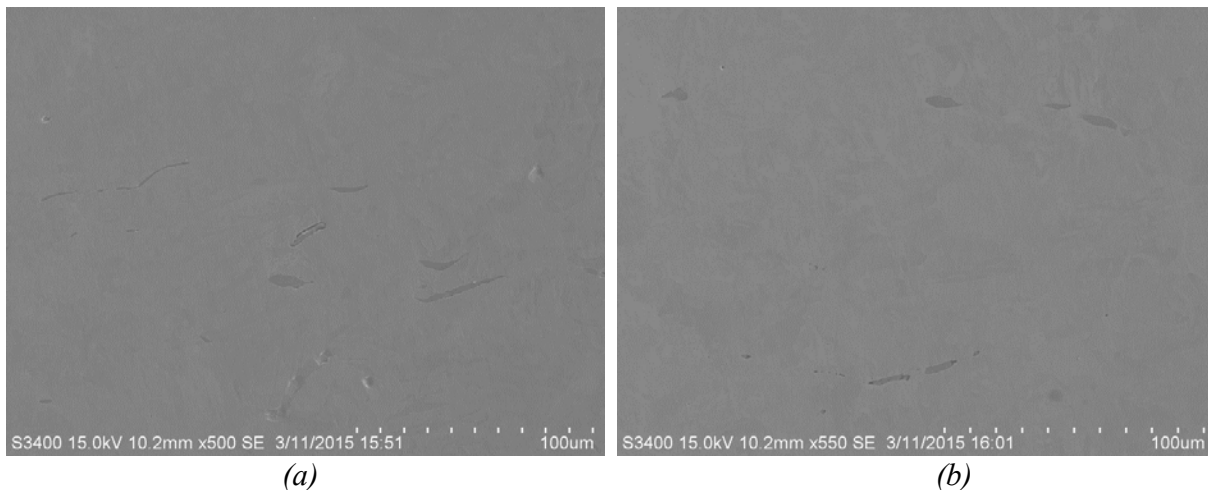


Figure 17. SEM micrographs of sample C (niobium added), 82° F superheat; 500X magnification

3.6. Discussion

The results of this work thus far indicate that there is a relationship between the superheat of steel (in the cast billet form), the chemistry, the rolling process, the cooling rate, and the microhardness of the steel. The rolling process and the cooling rate of the rolled product enable the evolution of appropriate microstructure. This work did not study the rolling process. Hence any contribution from superheat in the hardness discussion would only be tangential or conjectural since the equiaxed zone, which is most influenced by superheat, is readily collapsed or lost in the rolling process. The influence of superheat is most evident in cast billets but not in rolled products. This work was on rolled products.

Steels cast at high superheat could still make good products but must be rolled with high reduction ratios to achieve this aim. High superheat cast products without high reduction ratios could lead to more evidence of center line segregation.

Another observation that was made was that there was no significant evidence of macrosegregation in the samples. This is so because the samples were from rolled products and not from the cast billets. The center line had been completely removed by the rolling process. Efforts taken to see macrosegregation included cutting the samples into two halves, and in some cases machining the samples to the center of the 0.75" diameter bar. In either case, no evidence of segregation was noted. This was evidence that the rolling process removed the segregation in spite of the starting superheats in the billet form.

One major advantage of superheat control is reduction in kWh/ton. A plot of such a benefit obtained from an operating mill is shown in Fig. 18.

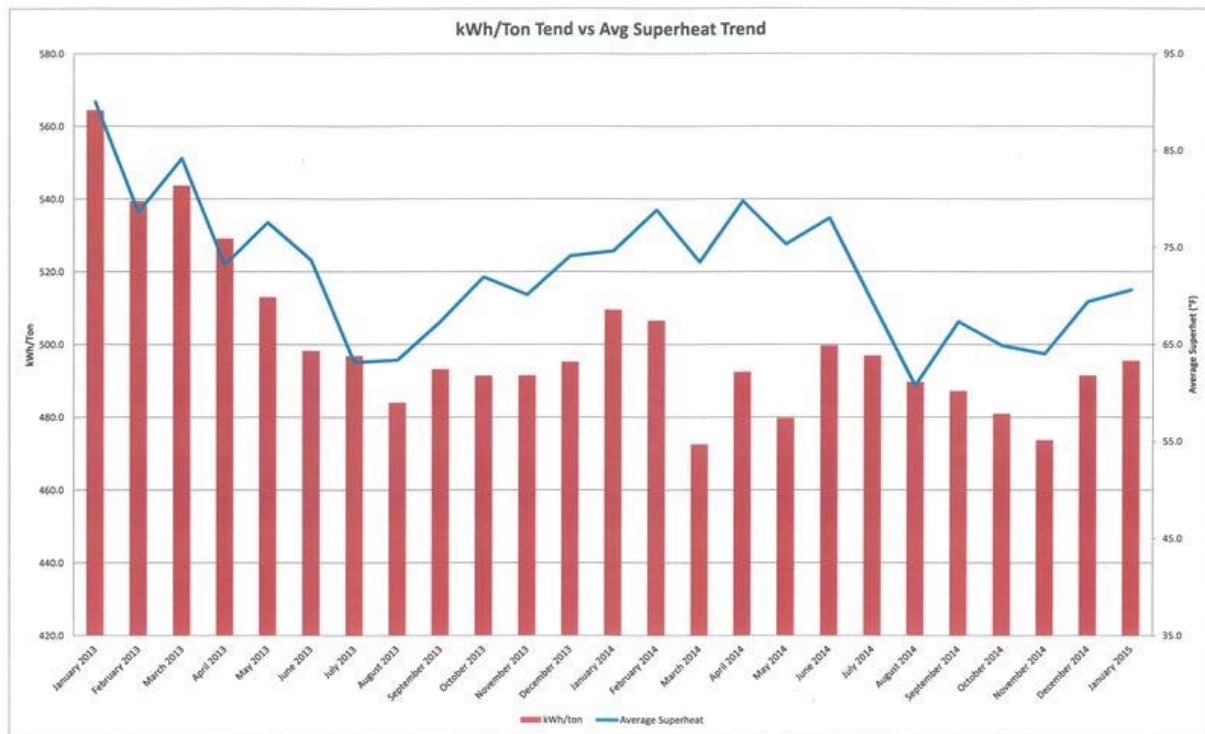


Figure 18. Plot of KWH/Ton versus superheat in actual mill setting [13]

Physical test results of the three steel samples show that they all meet ASTM Grade 60 specifications. Production cost (following quality) is always essential in alloy design. Minimization of the cost of alloying elements is a major consideration in steel making, more so in today’s market where construction bars are certainly a commodity and cheap bars flood American markets from Asia, the Middle East, and the Americas. Mills are therefore intent on making quality steels without spending too much on alloying elements but taking advantage of the metallurgy of tramp elements in the scrap mix.

The similarity of the physical test results derive from a couple of points. One important reason is that each rolling was done at a high enough temperature to ensure that the RDR process was established followed by air cooling. A second possible reason is suggested to be from the amount of residual molybdenum in the scrap mix. Even though the molybdenum (Mo) residuals are identical, its presence in the alloy is advantageous for high temperature strengthening. Andrade et al. [7] reported that Mo was next in line to niobium in retardation of static recovery and recrystallization. Molybdenum also contributes to hardenability and suppresses the formation of diffusional transformation products such as ferrite or pearlite in favor of bainitic and martensitic transformations, which are known as to be non-diffusional. The authors studied the high temperature strengthening produced by additions of molybdenum, niobium and vanadium using the empirical equation proposed by Akben et al. [8] as in equation (1) below,

$$\Delta S_a = \frac{\sigma_{ys} - \sigma_{ys}^{PC}}{\sigma_{ys}^{PC}} \times \frac{0.1}{at.pct S} \times 100 \quad (1)$$

where, σ_{ys} represents the yield stress of the steel and s the element under consideration; σ_{ys}^{PC} is the yield strength of the reference plain carbon steel.

Table 5 shows results from Andrade and co-workers [7] on the high temperature strengthening produced by additions of molybdenum, niobium, and vanadium.

Table 5. High temperature strengthening produced by additions of Mo, Nb and V in the steel [7]

Steel	σ_{ys} (MPa)*		Element	ΔS_s (per 0.1 at. pct)	ΔS_w (per 0.1 wt pct)
	1000 °C	900 °C			
Plain C	35.5 ± 1.4	40.6 ± 2.5	—	—	—
V	38.0 ± 2.4	44.0 ± 1.3	V	7.2	7.9
Mo	39.0 ± 1.8	56.2 ± 1.7	Mo	15.2	8.9
Nb-Mn	50.0 ± 1.8	58.5 ± 1.6	Nb	212.0	127.0

This Table 5 shows that niobium has the greatest strengthening effect followed by molybdenum and then vanadium. High residuals of molybdenum in a scrap mix are therefore an advantage to exploit.

In order to generate a predominantly bainitic microstructure, accelerated cooling has to begin above the temperature at which austenite transforms to ferrite. This is at above the A_{r3} temperature. Molybdenum is known to lower the A_{r3} temperature more effectively than addition of the same quantities of copper, nickel or chromium [9, 10]. Usually molybdenum levels of 0.2% or above are used in high strength line pipe steels. Llopsi [11] showed that a combined addition of chromium and molybdenum is more effective in promoting bainite formation than an addition of only one of the elements. Stallybrass and co-workers [12] showed that use of as little as 0.1% Mo and 0.2% Cr in making X80 sheet steel met the desired strength. Since the Cr and Mo levels in the current work (Table 1) are comparable and since the steel being produced is of lower strength that of the Stallybrass et al. work, it is not surprising to expect that higher strength levels.

In summary, new grade development success differs from mill to mill and truly depends on a mills specific culture and capabilities to achieve desired results. That success necessitates a thorough understanding of melting and secondary metallurgy reheat furnace characteristics, along with the mill’s cost drivers, culture, and commitment from leadership to support something new.

Summary. The major conclusion from this work is therefore that making steel for requisite standards like ASTM 615/A615M Grade 60 may not be dependent on starting superheat but on the chemistry and rolling process. Study of the three chemistries indicated as A, B and C indicate that the standard was met in all three chemistries but that sample A had the lowest cost chemistry and therefore is a suggested route for this product.

Acknowledgements

The authors are grateful to Nucor Corporation for the generosity and provision of the Nucor NERC facilities located in Tuskegee University. The authors are also grateful to Tuskegee University for the use of its facilities and equipment. Assistance received from Jerome Jones, an undergraduate student of mechanical engineering at Tuskegee University, in laboratory works is greatly appreciated. Nucor Steel Marion, OH is truly appreciated for the supply of all the grades of steel used in this work.

References

- [1] Pickering, F.B., 1967, The structures and properties of bainite in steels. Paper presented at the Symposium: A transformation and hardenability of steels, February 27-28th in Ann Arbor, MI. pp. 109-132.
- [2] deBoer, H., Datta, S.R., Kaiser, H.J., Lundgren, S.O., Müsgen, B., Schmedders, H., Wick, K., 1995, Naturharte bainitische Schienen mit hoher Zugfestigkeit, in: *Stahl and Eisen* 115, 93ff.
- [3] Mesplont, C., 2002, Phase Transformations and microstructure-mechanical properties relations in Complex Phase high strength steels. Doctoral Thesis, Ingénieur Ecole Universitaire Des Ingénieurs de Lille DEA Science des Matériaux Université de Lille, Universiteit Gent.
- [4] Maynier, P., Dollet, J., Bastien, P., 1978, Hardenability Concepts with Applications to Steels, D.V. Doane and J.S. Kirkaldy, eds., AIME, New York, NY, p.518.
- [5] Donnay B., Herman J.C., Leroy V., Lotter U., Grossterlinden R., Pircher H., 1996, Microstructure evolution of c-mn steels in the hot deformation process: the STRIPCAM model, Proc. Modelling of Metal Rolling Processes Conf., eds. J.H. Beynon, P. Ingham, H. Teichert, K. Waterson, London, pp. 23–35
- [6] Lagneborg, R., Siwecki, T., Zajac, S., Hutchinson, B., 1999, The Role of Vanadium in Microalloyed Steels, *The Scandinavian Journal of Metallurgy*, October, Vol 28, No 5, pp. 186-241.
- [7] Andrade, H.L., Akben, M.G., Jonas, J.J., 1983, Effect of Molybdenum, Niobium and Vanadium on Static Recovery and Recrystallization and on Solute Strengthening in Microalloyed Steels, *Metallurgical Transactions A*, Vol. 14 A, pp. 1967 – 1977.
- [8] Akben, M.G., Weiss, I., and Jonas, J.J., 1981, Dynamic Precipitation and Solute Hardening in AV Microalloyed Steel and two Nb Steels Containing High Levels of Mn, *Acta Metallurgica*, vol. 29, pp. 111-121.
- [9] Klinkenberg, C. Niobium in Microalloyed Structural and Engineering Steel (Niobium Products Company GmbH, Steinstrasse 28, D-40210 Düsseldorf, Germany)
<http://www.metal.citic.com/iwcm/UserFiles/img/cd/2005-HSLA-NB/HSLA-045.pdf> (accessed September 14th 2015)
- [10] Ouchi, C., Sampei, T., and Kozasu, I., 1982, The effect of hot rolling condition and chemical composition on the onset temperature of γ/α transformation after hot rolling, *Transactions of the Iron and Steel Institute of Japan*, 22, pp. 214–222.
- [11] Llopis, A.M., 1975, Effect of Alloying Elements in Steels on the Kinetics of the Austenite to Bainite transformation, (DOE Technical Report, DOI 10.2172/7283325, California University.
- [12] Stallybrass, C., Konrad, J., and Meuser, H., 2015, The Effect of Low Levels of Molybdenum in High Strength Linepipe Steels, *Fundamentals and Applications of Mo and Nb Alloying in High Performance Steels*, Vol. 2, Hardy Mohrbacher (Ed.), NiobelCon, Belgium, pp. 125 – 140.
- [13] Quality Department, Nucor Steel Marion, Private Communication.